

Imaging of phenomena in the night atmosphere

Institute for Information Education, University of Edogawa, Komaki 474, Nagareyama, Chiba, Japan.

Tomoo AOYAMA¹⁾

Abstract

This is a technical report for the educational engineering for imaging in the thermal infrared wave. It is used to make programming of visualization, and introduction to environmental lectures.

Keywords: Himawari-8, infrared images, ground emission, Philippine Taal volcano, Australia forest fire

1. Object and the approach

Phenomena in the atmosphere do not always happen under the daylight. Observations of night atmosphere are difficult. But, we believe they are necessary, and make imaging in the thermal infrared waves.

National Institute of Information and Communications Technology (NICT) and Meteorological Agency (JMA) in Japan [1] operate a geostationary satellite “Himawari-8” for observing atmospheric status, and publishes data per 10 minutes every 24 hours. We can browse the images without the application. They are published as a data base (DB) [2].

It has 16 bands and 3 viewers. The band characters are listed in Table 1.

The night images are got under a viewer for 3.9-13.3 μm. The image look like full color, but it is illusion; that is built in color mapped on a terrain map. Atmosphere information is in the white hazy patterns. Another visual image viewer gives true full color images, and the resolution is higher than that of 24 hours one.

Visual images are represented by png-format, which can be downloaded from the link in the viewer. Since infrared images cannot do so, we get them via screenshots.

Table 1. Characters of 16 bands and 3 viewers

	Wave length	Characters, Viewers* Characters	Our selection
1	0.47063 μm	visual image, *Japan, half-earth	C0(B)
2	0.51000	Visual image, *Japan, half-earth (center is 140.7 E)	C0(G)
3	0.63914	visual image, *Japan, half-earth	C0(R), C1(R)
4	0.8567	From here near infrared (NIR)	C1(G)
5	1.6101	Vegetation, aerosol, ice drop clouds	C1(B)
6	2.2568	Until NIR, No night image until the band, cloud phase	
7	3.8853	24h detection from here, low layer clouds, mist, natural fire	C4
8	6.2429	Upper layer vapor	C2(B)
9	6.941	Upper~middle layer vapor	C2(G)
10	7.3467	Middle layer vapor	C2(R)
11	8.5926	Thermal emission band from here, clouds phase, SO ₂	C3(B)
12	9.6372	Ozone	C3(G)
13	10.4073	From here, thermal infrared band, clouds images, no lower clouds	C4
14	11.2395	Clouds, sea surface temperature	
15	12.3806	Clouds, sea surface temperature	
16	13.2807	Clouds top	C3(R)
	↑[3]	*24 hours viewer accesses all bands.	

Since some imaging approaches in infrared region can be defined, we classify them into 4-kinds, C1~C4. The band-widths are 1.0, 1.1, 4.7, and 6.5 μm , respectively. The C0 (0.3 μm) is the visual image. Our selected colorings have wide band width compared with the visual.

The C1 is to detect ice-particles in upper-layer of clouds. The order of RGB is reversed to visible light to make the cloud-ice be blue. The C1 is useful; however, it is not adopted in night.

The C2 is to find diffuse moisture distributions in upper~middle layers air. It is used for detection of large scale vortexes in air. From the coloring, the night imaging is enabled.

The C3 is an analogy of C0-selection; it finds the difference of clouds in thermal infrared waves. Spectra of SO_2 and O_3 gases are in the region. Since their intensity is weak against that of H_2O , the effects are detected indirectly. Even if setting C3(R) of 10.4 μm , generating image is not so different.

The C4 is to detect difference of clouds in the upper and lower layers. The C4 is not based on 3 primary colors but pseudo-color of subtraction of 2 bands. See document [4] for the reason, please.

To make night color images, we must get 4 screenshots from the 24 hours viewer. One is a terrain map as the background. The other 3 are selection for user's projects. We discuss (1) extraction of the white hazy pattern on background, and (2) brightness matching among the 3 extracted monochrome haze images.

2. Extraction of white hazy pattern

2.1 Wave dependency ratio {wR, wG, wB}

3 standard wave length set, $\{R_\lambda, G_\lambda, B_\lambda\}$, is defined, and the dependency factor (n) is given.

$$fR=1/R_\lambda^n, fG=1/G_\lambda^n, fB=1/B_\lambda^n; w=\min(fR, fG, fB); \quad (1)$$

$$wR=w/fR, wG=w/fG, wB=w/fB. \quad (2)$$

Since we adopt final results to be human vision, $\{R_\lambda, G_\lambda, B_\lambda\}=\{0.63, 0.55, 0.45\}$ [μm]. The "n" is set as "0<n<3". If the pure Rayleigh scattering is observed, it is n=4. Empirically, it is n=1.5~2.5.

2.2 Logical function to extract white pattern

As each pixel expressed by $\{R_{ij}, G_{ij}, B_{ij}\}$,

$$w=\min(R_{ij}, G_{ij}, B_{ij}), \text{ and } \{dR_{ij}, dG_{ij}, dB_{ij}\}=\{R_{ij}-w, G_{ij}-w, B_{ij}-w\}. \quad (3)$$

In this paper, the value of each pixel is the real number. A threshold "th" is introduced, and a condition is defined.

$$L(\text{th})=\text{Logical}(dR_{ij} < \text{th}/wR \ \& \ dG_{ij} < \text{th}/wG \ \& \ dB_{ij} < \text{th}/wB), \quad (4)$$

Where "&" is logical and and-operator. Eq.(4) is a logical function.

If L(th) is true; then we set each pixel is, $\{R_{ij}, G_{ij}, B_{ij}\}=\{u, u, u\}$, $u=(R_{ij}+G_{ij}+B_{ij})/3$. (5A)

If L(th) is false; we set $\{R_{ij}, G_{ij}, B_{ij}\}=\{uR_{ij}, uG_{ij}, uB_{ij}\}$, $u=0.007$ (constant). (5B)

"th" of Eq.(4) is 20, it is got empirically. As the terrain map has green color; L(th)=false is got under the Eq.(4). By Eq.(5B), very small image information is remained. This is effectively when the negative pattern is reused. The extraction is not so good for weak haze; however, if the background is not, the approach is adopted.

Conversely, to reduce white, renew $\{R_{ij}, G_{ij}, B_{ij}\}=\{w*q+dR_{ij}, w*q+dG_{ij}, w*q+dB_{ij}\}$, $0<q<1$. This is a color-enhancer. Using the "q", we make coloring of white clouds, in order to detect SPM.

2.3 Subtraction of background

A background terrain pattern is the band-3 in the night, which is a color image. We write it, $\{R_{ij}', G_{ij}', B_{ij}'\}$. When an observation is written as, $\{R_{ij}, G_{ij}, B_{ij}\}$, following subtraction,

$$R_{ij}''=R_{ij}-s*R_{ij}', G_{ij}''=G_{ij}-s*G_{ij}', B_{ij}''=B_{ij}-s*B_{ij}', \quad (6)$$

is expected as white hazy pattern. It is true in case of s=1, when observation is added linearly on the background. However, on processing on the band-13, we get clouds pattern on the ground that is colored by magenta (complimentary of green). Moreover, we detect difference among tones for clouds over the ground and sea. *The addition is not linear.* To minimal the coloring and tone-difference, we get:

$$"s=1.025", \text{ if } R_{ij}'' < 0 \text{ then } R_{ij}''=0, \text{ if } R_{ij}'' > 255 \text{ then } R_{ij}''=255, \text{ same as } G_{ij}'' \text{ and } B_{ij}'' \text{".} \quad (7)$$

$$w=\max(R_{ij}'', G_{ij}'', B_{ij}''), \text{ renew } \{R_{ij}, G_{ij}, B_{ij}\}=\{w, w, w\}. \quad (8)$$

Eq.(7,8) is an approach by forcing to monochrome images.

The approach is effective, but small effects from the background are remained. Therefore, using plural snapshots, we must judge that a noisy small pattern is real or not. Since there is no physical background for processing of Eq.(7,8), when examining physical property of nighttime clouds, we stop the processing until Eq.(6). On the C4-color, we process images under Eq.(6).

3. Brightness matching

Average brightness of each band is not equal. If we composite 3 bands images simply, it would be strange one that is emphasized by one of 3 colors. There is no basis in synthesizing color images physically. Animals evolved to detect colors to process complex phenomena at high speed. So, to use the 3 primary color spaces efficiently, average brightness of each color is balanced.

We define following sigmoid functions;

$$\text{Sigmoid}(x)=1/[1+\exp\{-A(x-c_0)\}]=k \text{ (const.)}, \quad (9)$$

$$A=-\{1/(x-c_0)\} \text{Ln}\{(1/k)-1\}, \quad (10)$$

Where c_0 is a center of sigmoid-function, which is 127.5 in case of 8-bits. The “ k ” is constants, we adopt $k=\{0.1,0.9\}$. They correspond with brightness 1 and 254.

We define a finite sigmoid-function;

$$\text{Fsigmoid}(x)=\{0 \text{ (} x < 1), =1/[1+\exp\{-A(x-c_0)\}] \text{ (} 1 < x < 254), =1 \text{ (} 254 < x)\}. \quad (11)$$

This is a function that increases to the right between 1 and 254, with the center at 127.5.

We define an average of brightness $\text{AvgBr}()$, that is;

$$\text{AvgBr}(R)=\{1/\text{Fsigmoid}(c_0)\} \{\sum_{ij} R_{ij} \times \text{Fsigmoid}(R_{ij})\} / \{\sum_{ij} 1\}, \quad (12)$$

Where \sum_{ij} in Eq.(12) is in the defined area. The number of pixels is $\{\sum_{ij} 1\}$. This is a kind of averaging with weight. Icons of Himawari-8 viewer are excluded from the defined area. Then, 3 scalar variables, $\text{AvgBr}(R)\sim\text{AvgBr}(B)$, are calculated. As haze or clouds images, $\text{AvgBr}(R)\sim\text{AvgBr}(G)\sim\text{AvgBr}(B)$ is expected.

We believe a balancing of each band is;

$$w=\min\{\text{AvgBr}(R), \text{AvgBr}(G), \text{AvgBr}(B)\},$$

$$\text{Bi}(R)=\text{AvgBr}(R)-w, \text{ Bi}(G)=\text{AvgBr}(G)-w, \text{ Bi}(B)=\text{AvgBr}(B)-w, \quad (13)$$

$$ww=R_{ij}-\text{Bi}(R); R_{ij}=0 \text{ (} ww < 0), R_{ij}=ww \text{ (} 0 < ww < 255), R_{ij}=255 \text{ (} 255 < ww). \quad (14)$$

G_{ij} and B_{ij} are calculated samely.

4. Display brightness adjustment

After image processing under floating points, since the RGB-space is over 8-bits, we project it to a 8-bits space. The R_{ij} is,

$$\text{proj}(R_{ij})=[\text{amp} \times R_{ij}-\text{bi}], 0.5 < \text{amp}. \quad (15)$$

When $\text{proj}(R_{ij})$ is under 0 or over 255, the values are set to be 0 or 255. The “ bi ” is a bias-parameter, which is adjusted by checking images. The “[\cdot]” is Gauss symbol.

We run imaging programs with a RGB-viewer parallely. We use “Daisy Collage ® [5]”. The $\text{proj}(G_{ij})$ and $\text{proj}(B_{ij})$ are calculated by using Eq.(15). The “ amp ” and “ bi ” are that

of R_{ij} .

Under Eq.(15), sometimes images are strong bluish or has brightness slope. Especially, in case of sunset or dawn (because of the sunlight is horizontal direction), the slope is large. But, 3D character of targets can be detected clearly. We compensate the sunlight angle. After those compensations, the inclination of color hue is found, we correct it in case of $C1\sim C3$ color by using Eq.(2), we redefine;

$$\text{proj}(R_{ij})=[wR \times \text{amp} \times R_{ij}-\text{bi}-\text{bN}/M-\text{bE}/N], \text{ proj}(G_{ij})=[wG \times \text{amp} \times G_{ij}-\text{bi}-\text{bN}/M-\text{bE}/N],$$

$$\text{proj}(B_{ij})=[wB \times \text{amp} \times B_{ij}-\text{bi}-\text{bN}/M-\text{bE}/N]. \quad (16)$$

The “ bN ” and “ bE ” are biases for vertical and horizontal directions. Bias parameters of Eq.(16) are 3 types. It is difficult to optimize these 3 kinds of biases; therefore, a RGB-image-viewer is required on parallel.

The “ n ” is a real number, $-0.5\sim 2.5$.

Eq.(16) is reasonable in the visual bands; however, in infrared bands, is it true? If we make adjustments between 3 colors that are not based on physical grounds, if we detect a characteristic pattern, it wouldn't there be any doubt about “existence of phenomenon”? Therefore; we introduce a restriction with Eq.(16), and consider with inheritance from visual band detected phenomenon that is observed before the sunset.

5. Diffusion of volcanic plumes

The Taal volcano in Philippines explodes at January 12, 2020. From Himawari-8 images, it can be confirmed that the plume rises at 16:00 JST (UTC+9h). The plumes rises to 15km [6]. The plume is spreading towards north direction. The visible image can be seen until 18:10. It is shown in Figure 1.

After that, the status of the plume is not visible until January 13 at 7:30. We show the plume diffusion at 23:00 and 3:00 by using the C4 approach described in Sections 1-4. They are in Figure 2~4. Images under Eq.(6) are $\{R, G, B\}$, which has color-information. It is based on blue and yellow; that is a pseudo-color. Stronger radiation of objects is darker pattern. Since it is a nega representation, we convert it to positive one. Therefore, upper layer clouds are yellow, and lower ones are blue. The plume over 10 km is very dark, thus, the positive image becomes whitey yellow.

To get full color images based on 3 prime colors, we test effects of the brightness matching in section 3. The targets are Taal's plumes at 18:20 and 20:00 JST.

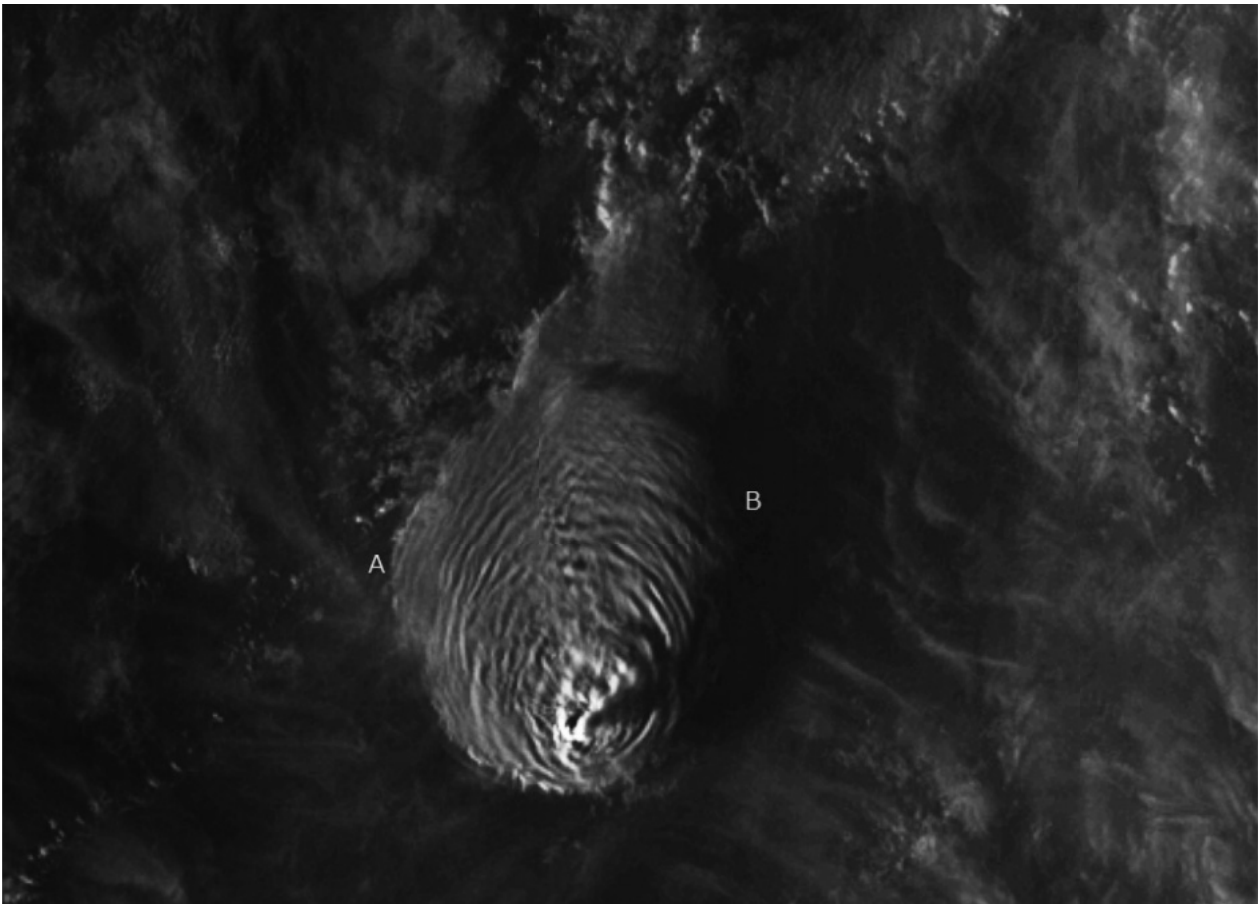


Figure 1. A visible image of Taal Volcano plume at 18:10 JST, January 12, 2020.

Original is full-color, where detail difference of the plume is found. Notice (1) you can see the sunset of the lower clouds through the plume at A; (2) It is seen the shadow of the volcanic plume 15 km high at B; (3) The difference in shape between the plume and normal clouds is found.

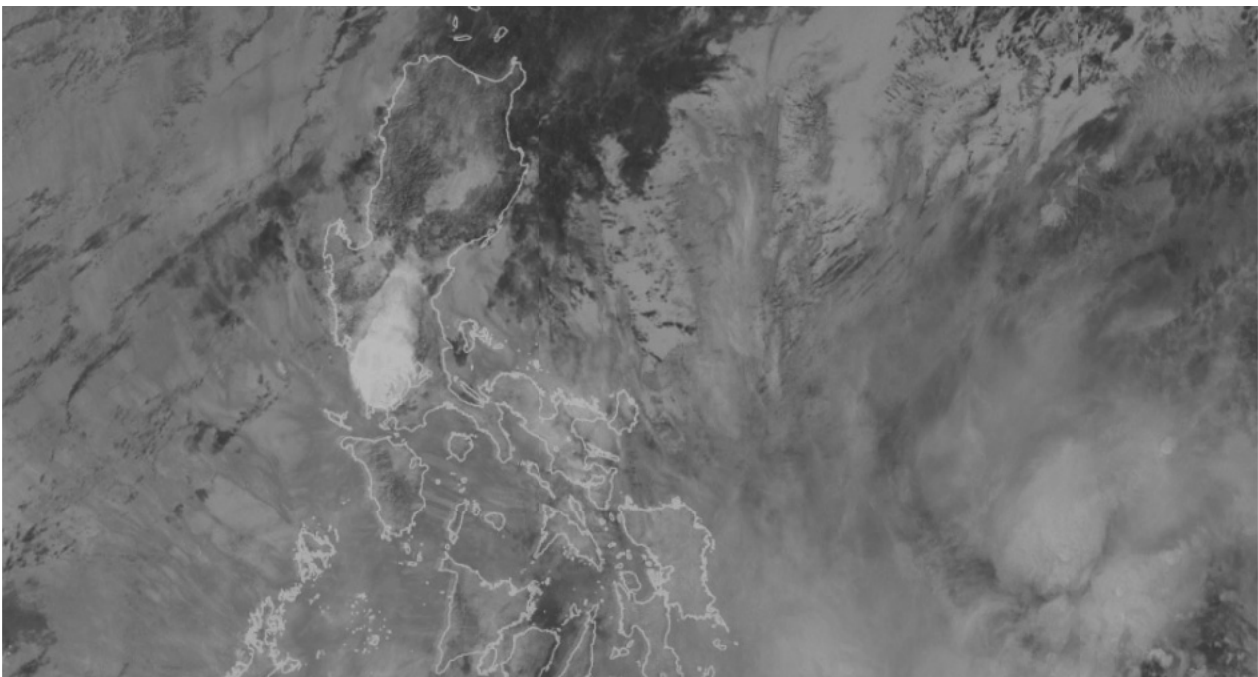


Figure 2. Plume of the Taal volcano at 18:00 JST, Jan. 12, 2020.

The original is C4-pseudo-color image, whose physical meaning is a subtraction and negative image between Band-7 and 13. Clouds in upper-layer are colored by yellow, and lower ones are blue.

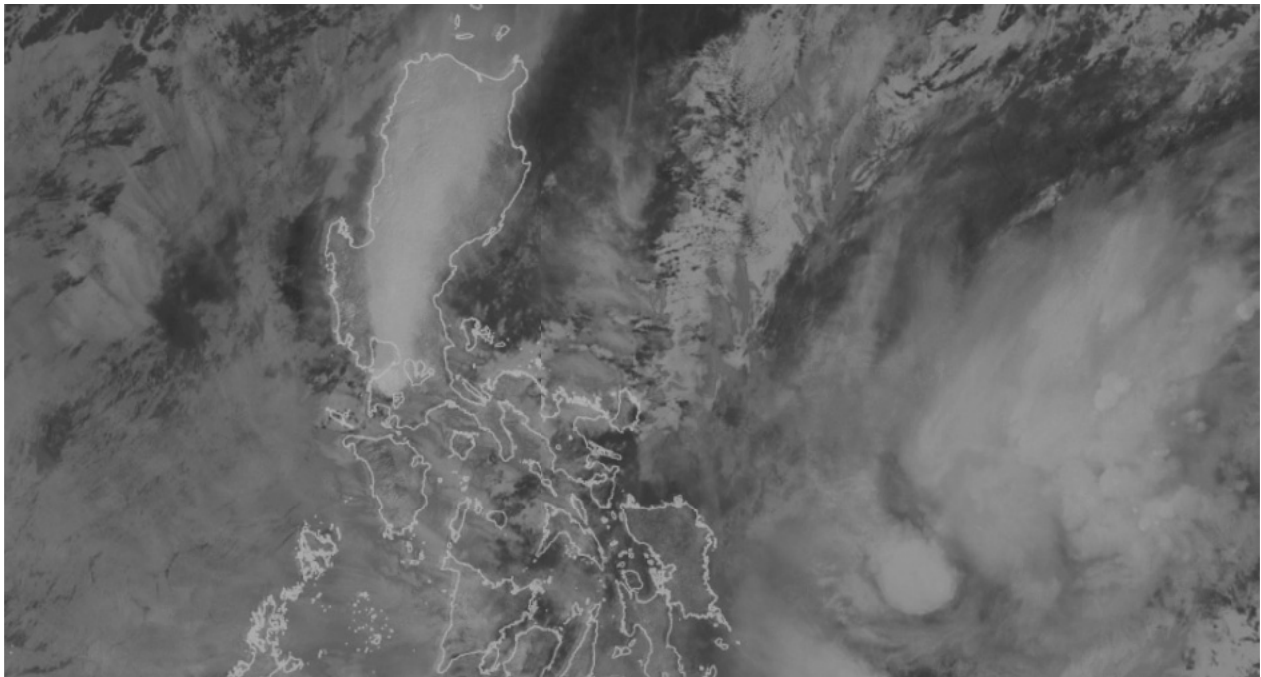


Figure 3. Plume of the Taal volcano at 23:00 JST, Jan. 12, 2020.

At that time, the plume closes to the property of normal clouds in upper-layer.

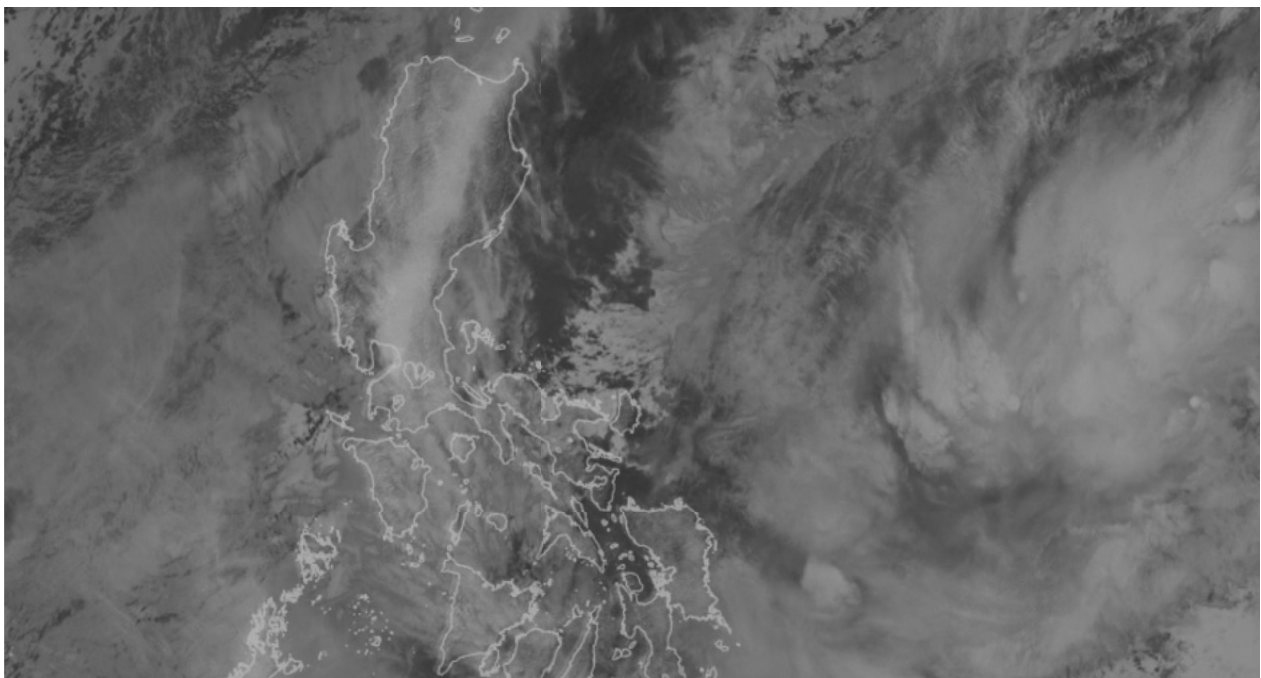


Figure 4. Plume of the Taal volcano at 3:00 JST, Jan. 13, 2020.

7. Significance of the imaging approach

We know many terrestrial events in the media and SNS. They are information that is unilaterally given to us. We want to confirm their truthfulness. We have no political power, no wealth, and no connections. Under such bad conditions, the truth of information is examined using satellite images.

The global catastrophe from late 2019 to early 2020 is the Australian forest fire. On December 31, fire smoke reached to New Zealand. It is shown in C1 color.

This is a visual image (C0 color). The forest fire (A) continues even on January 25! You can see the smoke (D) drifting over the sea far from Australia. The “B” is clouds generated from the smoke particles, and “C” is dust around

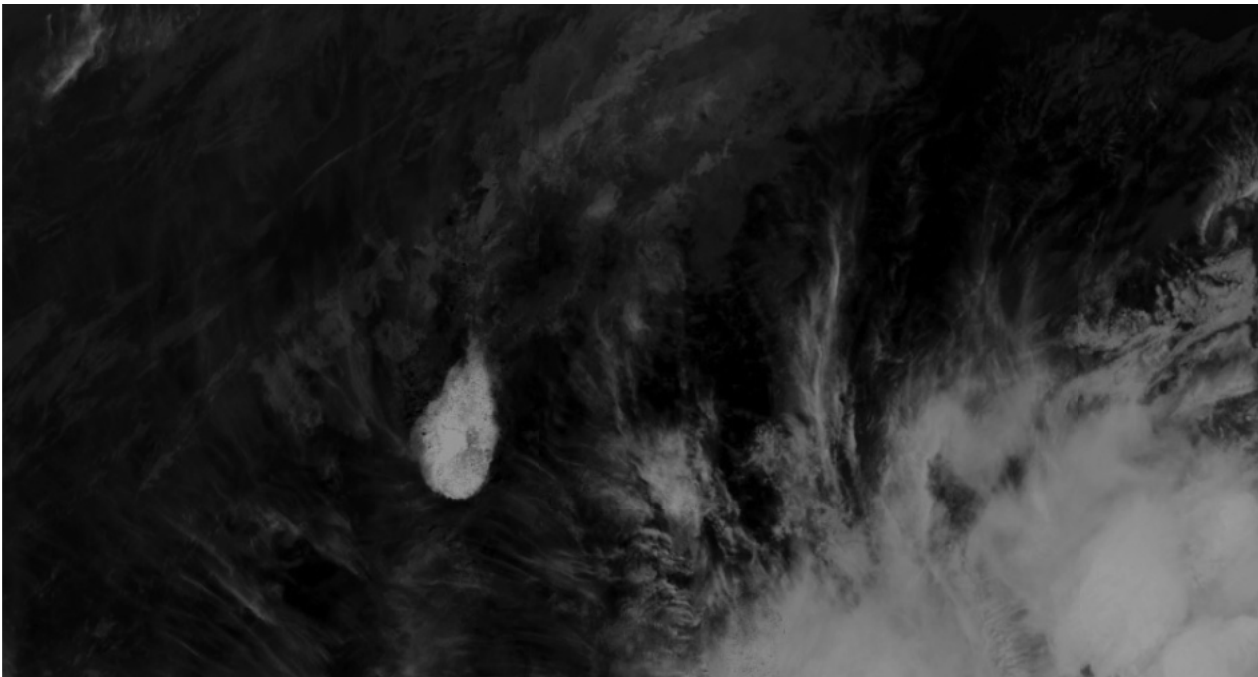


Figure 5. Plume of the Taal volcano at 18:20 JST, Jan. 12, 2020.

The original is C3-color image. We believe the color balance is satisfied. In lower right direction, you can see that there is a depression in the plume due to east winds.

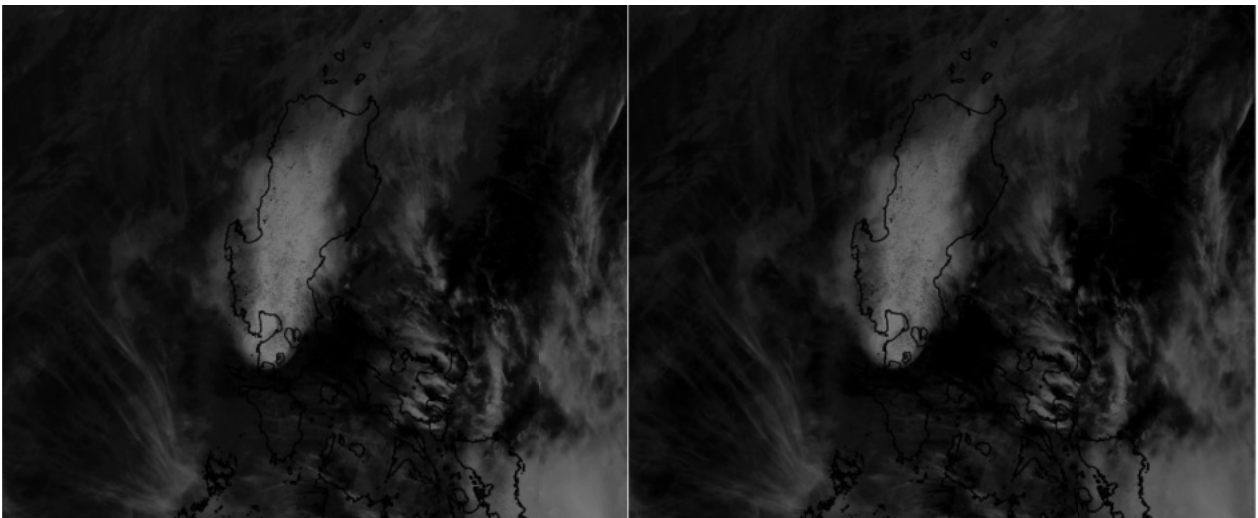


Figure 6. Plume of the Taal volcano at 20:00 JST, Jan. 12, 2020.

The images are C3-color, and the right is $\{8.6, 9.3, 13.3\}$ μm image. This is a test to check the difference between 10.4 and 13.3 μm . We believe the color balance is satisfied. Both images are almost equal. Sand spots in the plume are contamination noises from the background. Researching time-series screen shots, they are determined.

the clouds. The image is enhanced by techniques of reference [7].

Along with the forest fire, a sandstorm is occurring in the desert of central Australia.

We have imaged a plume of the Raikoke island, at June 22, 3:00 JST, in 2019. Many plumes are found until 15:00 at that day, and they flow towards the Bering Sea. The images are publish in SCCJ 2019 [8].

8. Conclusion

We develop a program for color imaging of the night atmosphere. It is to visualize between 3.9~13.3 μm , and is to research the vapor distribution in air. By the detected moisture patterns, movements of volcano plumes or forest fire smokes can be known indirectly.

We believe the program is useful tool for the environmental science. The advantage is that original

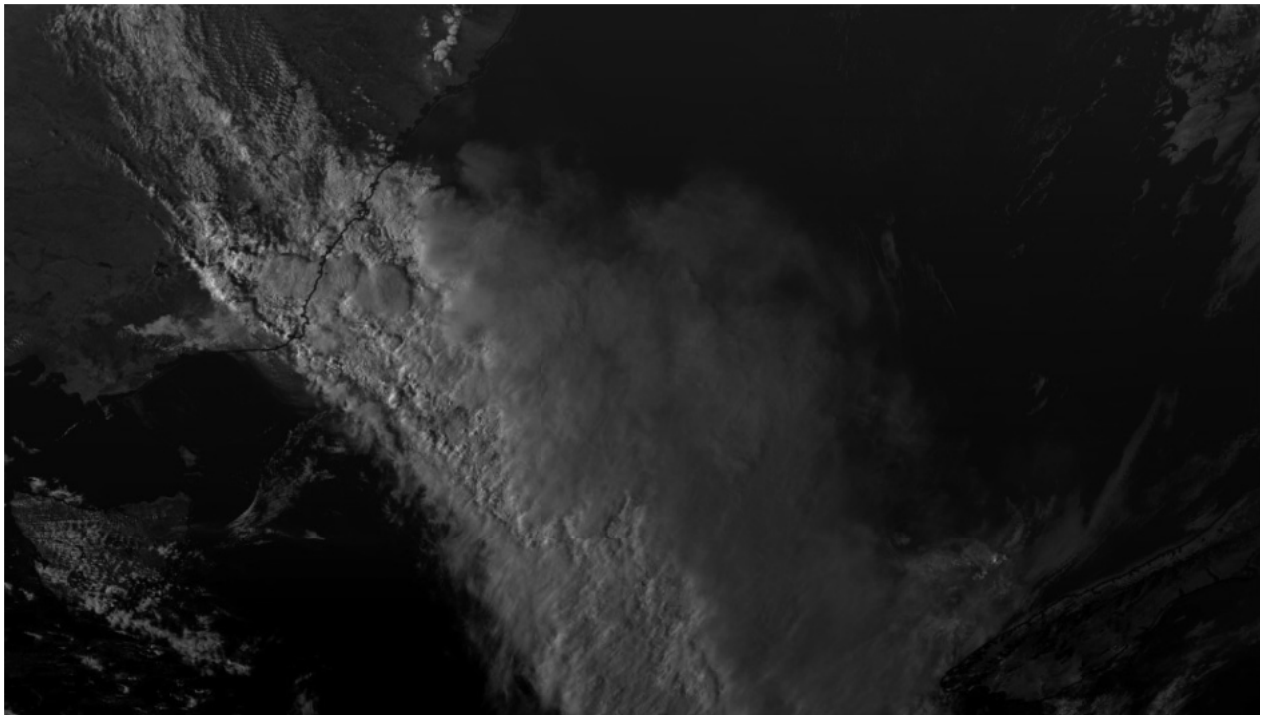


Figure 7. Fire smoke (gray) reached New Zealand (dark green, right down); December 31, 15:00 JST, 2019. The wildfire smoke (center, left-end, gray) is spreading northeast through ordinary clouds (yellow).

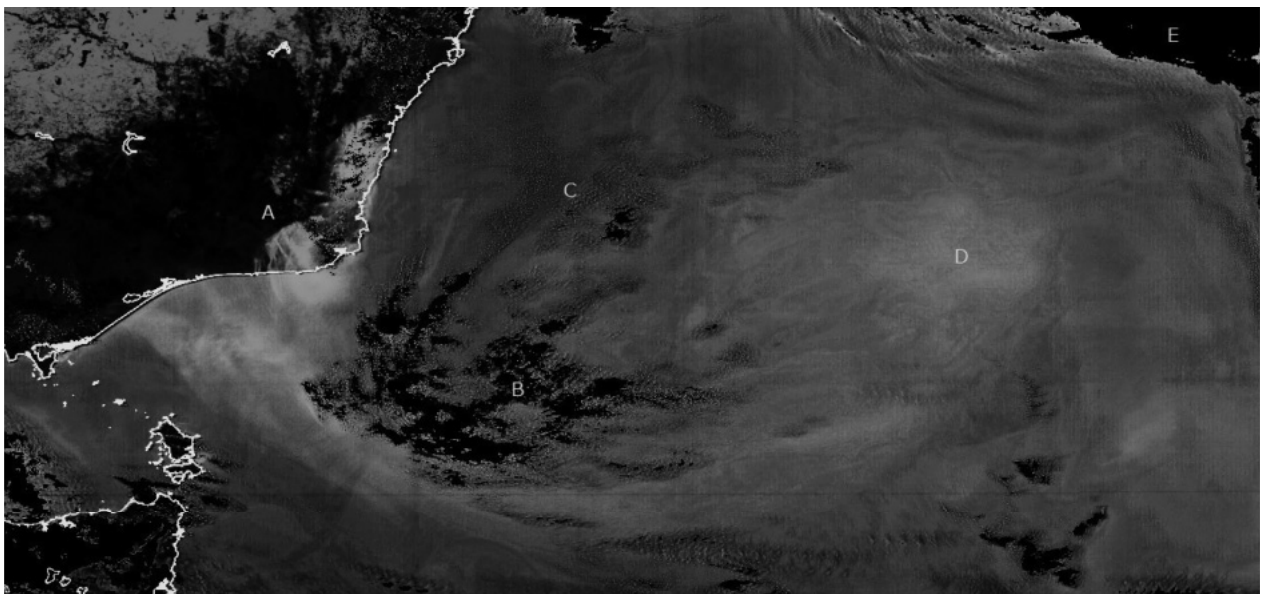


Figure 8. Four composited image during 12:20~12:50 JST, January 25, 2020. A: Forest fires, B: Clouds, C: SPM around clouds, D: Smoke of the fire having complex vortex.

images can be obtained via screenshots from the NICT general viewers.

9. Acknowledgment

We quote the WSDBank* Web developed by NICT** science cloud.

*World Science Data Bank, **National Institute of

Information and Communications Technology.

We are very thanks for allowance to access permission.

On January 9, 2020, a workshop was held at University of Edogawa to examine the global environment using screenshots and images of Himawari-8. All images in this paper are full-color. Due to the limitations of the academic repository, they are represented as the monochrome. Many

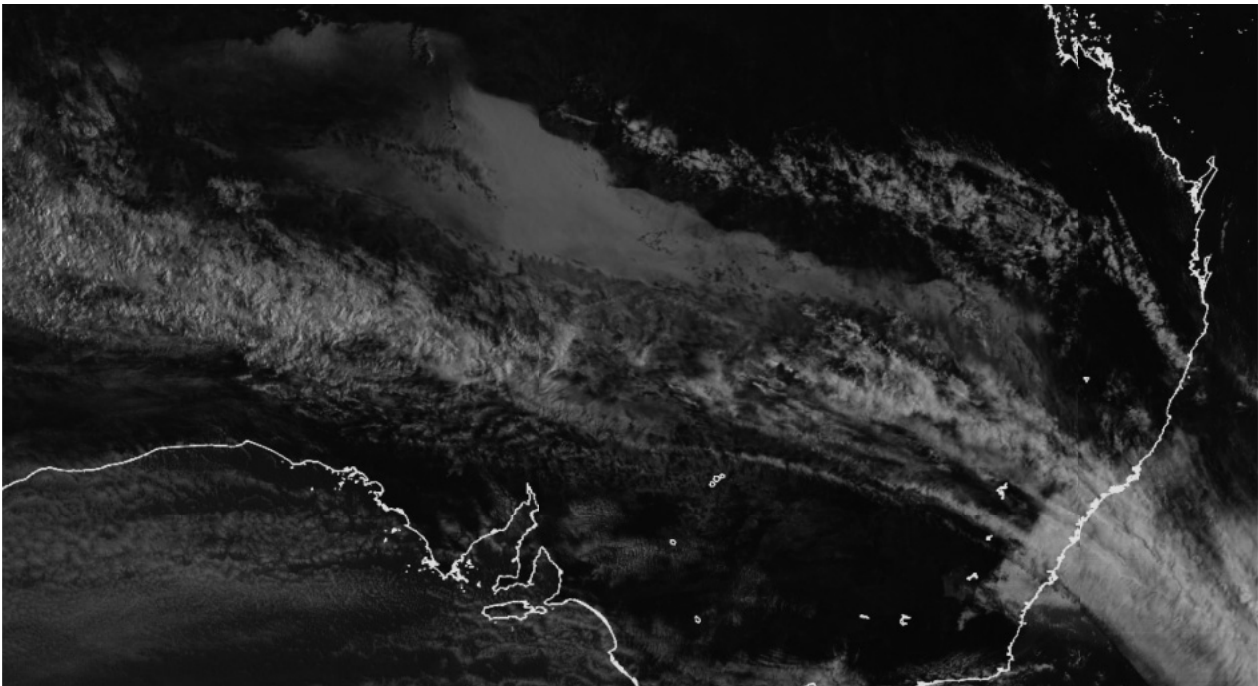


Figure 9. Sandstorm at 8:00 JST, January 11, 2020. Forest fire is seen at right-below. This is a visual image.

details have been lost.

10. References

- [1] Japan Meteorological Agency (JMA), <https://www.jma.go.jp/jma/indexe.html>.
- The satellite images: <https://www.jma.go.jp/jp/gms/largec.html?area=0&element=1&time=202001251720&line=0>.
- [2] Himawari-8 Real-time Web -NICT, <https://himawari8.nict.go.jp/>
- [3] Meteorological satellite center, “Advanced Himawari Imager (AHI)”, http://www.data.jma.go.jp/mscweb/ja/info/spsg_ahi.html.
- [4] A technical report (in Japanese) of Meteorological Satellite Center of JMA, “Basics of meteorological satellite observation and utilization of multi-band observation of Himawari-8.”, “Familiar satellite images reaffirm what you are observing.”, <https://www.jma.go.jp/jma/kishou/minkan/koushu160801/shiryou1.pdf>.
- [5] Daisy Collage 10 personal, Sourcnext®, https://www.sourcnext.com/product/pc/use/pc_use_000766/
- [6] Wether news 2020.1.12, 22:36 JST; “Philippines, Taal Volcano”, <https://weathernews.jp/s/topics/202001/120135/>
- [7] T. Aoyama, T.Yagi, “Environmental information extracted from satellite images: Aspects of Sea and Atmosphere”, Edogawa University Repository, Informatio, vol.16; https://edo.repo.nii.ac.jp/index.php?action=pages_view_main&active_action=repository_view_main_item_snippet&index_id=65&pn=1&count=20&order=7&lang=japanese&page_id=13&block_id=21
- [8] K.Akashi, J.Kambe, U.Nagashima, T.Aoyama, “Development of status analyzer for the atmosphere: using global image of Himawari-8 (in Japanese)”, Society of Computer Chemistry in Japan (SCCJ) annual meeting 2019, Hiroshima, 2P23; <http://www.bio.info.hiroshima-cu.ac.jp/sccj2019/>.